

values and their assignments, it was necessary to try many assignments for each compound. The best fits were selected on the basis of physically reasonable values of k , δ , and ϵ .

Perusal of Table XIII shows that in all cases the value of B is very large which indicates that the ground-state Kramers doublet consists mainly of a state wherein the unpaired electron resides in the d_{xy} orbital. This is in agreement with our interpretation of the Mössbauer data. Another important result is that δ/ζ ranges between 6.8 and ca. 11.6. If the free-ion one-electron spin-orbit constant is taken as 460 cm^{-1} , δ ranges between 1500 and 4800 cm^{-1} . In other words, the energy difference between the ground-state Kramers doublet A' and the center of gravity of the two excited doublets (both A'') from the low-spin manifold is very large. This explains why it is easy to see EPR spectra even at room temperature, for it has been shown that the rate of spin-lattice relaxation ($1/T_1$) is proportional to $(\zeta^2 H_0^4 T)/\delta^4$, where H_0 is the magnetic field.⁴⁶

Conclusion

The series of compounds $[\text{Fe}(\text{X-SalEen})_2]\text{Y}$ has been shown to exhibit most all of the curiosities observed for spin-crossover complexes in the solid state. It is shown with EPR and ^{57}Fe Mössbauer data that regardless of the shape of the $\mu_{\text{eff}}/\text{Fe}$ vs. temperature curve only two states, the high-spin $^6A_{1g}$ and the lowest energy Kramers doublet from $^2T_{2g}$, are thermally populated for these compounds. There is no evidence for population of an intermediate-spin ($^4T_{1g}$) state. The

ground-state Kramers doublet has been characterized as d_{xy} .

Acknowledgment. The support of the National Institutes of Health under Grant HL13652 is gratefully acknowledged. Thanks are in order to Professor Peter Debrunner for the use of his Mössbauer instrumentation.

Note Added in Proof. A low-temperature ^{57}Fe Mössbauer spectrum was run for a sample of the essentially low-spin compound $[\text{Fe}(\text{3-OCH}_3\text{-SalEen})_2]\text{NO}_3 \cdot 1/2\text{H}_2\text{O}$ in the presence of a large (ca. 60 kG) longitudinal applied magnetic field. The appearance of a "doublet-triplet" pattern with the triplet at more positive velocities corroborates the conclusion reached in this work that $V_{zz} < 0$ for the low-spin $[\text{Fe}(\text{X-SalEen})_2]\text{Y}$ complexes. This conclusion was reached previously on the basis of the asymmetry of the quadrupole doublets at zero applied field.

Registry No. $[\text{Fe}(\text{SalEen})_2]\text{PF}_6$, 73261-28-6; $[\text{Fe}(\text{SalEen})_2]\text{NO}_3$, 73370-18-0; $[\text{Fe}(\text{3-OCH}_3\text{-SalEen})_2]\text{NO}_3$, 75112-21-9; $[\text{Fe}(\text{3-OCH}_3\text{-SalEen})_2]\text{BPh}_4$, 73261-30-0; $[\text{Fe}(\text{3-OCH}_3\text{-SalEen})_2]\text{PF}_6$, 73261-31-1; $[\text{Fe}(\text{5-OCH}_3\text{-SalEen})_2]\text{NO}_3$, 75112-23-1; $[\text{Fe}(\text{5-OCH}_3\text{-SalEen})_2](\text{PF}_6)_{0.5}(\text{NO}_3)_{0.5}$, 75112-24-2; $[\text{Fe}(\text{Saen})_2]\text{Cl}$, 75112-25-3; $[\text{Fe}(\text{5-OCH}_3\text{-SalEen})_2]\text{BPh}_4$, 75112-26-4; $[\text{Co}(\text{3-OCH}_3\text{-SalEen})_2]\text{PF}_6$, 75083-22-6; $[\text{Fe}(\text{SalEen})_2]\text{BPh}_4$, 75112-27-5; salicylaldehyde, 90-02-8; 5-methoxysalicylaldehyde, 672-13-9; *N*-ethylethylenediamine, 110-72-5; ethylenediamine, 107-15-3; 3-methoxysalicylaldehyde, 148-53-8.

Supplementary Material Available: Tables I-XI, magnetic susceptibility data (14 pages). Ordering information is given on any current masthead page.

Contribution from the School of Chemical Sciences,
University of Illinois, Urbana, Illinois 61801

Spin-Crossover Ferric Complexes: Unusual Effects of Grinding and Doping Solids

MUIN S. HADDAD,¹ WAYNE D. FEDERER,² MICHAEL W. LYNCH, and DAVID N. HENDRICKSON*

Received July 14, 1980

Magnetic Susceptibility, EPR, ^{57}Fe Mössbauer, and X-ray powder diffraction data are presented for the $[\text{Fe}(\text{X-SalEen})_2]\text{Y}$ series of ferric spin-crossover complexes to substantiate the presence of the nucleation and growth mechanism for the spin-crossover phase transition in solid samples of these complexes. The compound $[\text{Fe}(\text{3-OCH}_3\text{-SalEen})_2]\text{PF}_6$, where 3-OCH₃-SalEen is the monoanion of the Schiff-base condensation product from 3-methoxysalicylaldehyde and *N*-ethylethylenediamine, exhibits an almost discontinuous spin-crossover transition with a hysteresis of 2-4°. Grinding a microcrystalline sample of this compound leads to an incompleteness of the transition; some complexes persist in the high-spin state at low temperatures. The transition also becomes more gradual upon sample grinding, and more low-spin molecules form in the ground samples at higher temperatures compared to the unground samples. The temperature at which there are equal numbers of low-spin and high-spin molecules also shifts to a lower value upon sample grinding. The effects of sample grinding are found to be general for the $[\text{Fe}(\text{X-SalEen})_2]\text{Y}$ complexes and are most likely attributable to defects caused by the grinding. Physical data point to the presence of molecules in only two electronic states even for the ground samples. The results of a study of crystalline doped $[\text{Fe}_x\text{Cr}_{1-x}(\text{3-OCH}_3\text{-SalEen})_2]\text{PF}_6$ and $[\text{Fe}_x\text{Co}_{1-x}(\text{3-OCH}_3\text{-SalEen})_2]\text{PF}_6$ show that the effects of doping (e.g., more gradual transition) are very similar to those seen for sample grinding. In fact, grinding a doped sample leads to the most pronounced change. For the doped samples it is found on one hand that, as the chromium(III) concentration is increased, the transition temperature shifts to lower temperature, whereas on the other hand, as the cobalt(III) concentration is increased, there is a shift to higher temperature. An explanation of the various observations in terms of the nucleation and growth mechanism of phase transitions in the solid state is given. The results of some interesting EPR observations on these ground and doped $[\text{Fe}(\text{X-SalEen})_2]\text{Y}$ complexes are reported.

Introduction

In the preceding paper, variable-temperature magnetic susceptibility, EPR, and ^{57}Fe Mössbauer results were presented for the $[\text{Fe}(\text{X-SalEen})_2]\text{Y}$ series of ferric spin-crossover complexes. It was shown that the full range of unusual phenomena is seen for these spin-crossover complexes in the solid state. The temperature dependence of the magnetic susceptibility for a compound does not simply reflect a Boltzmann distribution over thermally populated states. In the case of many

compounds, the spin-crossover transformation does not go to completion as the sample temperature is decreased. Different preparations of a given complex exhibit appreciable differences in physical properties. No evidence of an intermediate-spin state was found.

It is our hypothesis that all of the curiosities observed for the spin-crossover complexes in the solid state can be explained by the general nucleation and growth mechanism of phase transitions in solids.^{3,4} The spin-crossover transformation is

(1) University of Illinois Fellow, 1976-1979.
(2) 3M Fellowship, 1979-1980.

(3) Rao, C. N. R.; Rao, K. J. "Phase Transitions in Solids"; McGraw-Hill: New York, 1978.

Table I. Analytical Data

compd	% C		% H		% N		% M	
	calcd	obsd	calcd	obsd	calcd	obsd	calcd	obsd
[Co(3-OCH ₃ -SalEen) ₂]NO ₃	51.14	51.82	6.04	6.20	12.43	12.21	10.46	10.49
[Co(SalEen) ₂]NO ₃	52.51	52.79	5.96	6.22	13.91	14.07	11.71	11.69
[Co(3-OCH ₃ -SalEen) ₂]PF ₆	44.61	43.95	5.61	5.17	8.67	8.51	9.12	9.09
[Co(SalEen) ₂]PF ₆	45.08	45.21	5.12	5.22	9.55	9.51	10.05	9.91
[Fe _{0.77} Co _{0.23} (3-OCH ₃ -SalEen) ₂]PF ₆	44.78	44.68	5.28	5.53	8.70	8.69	Fe 6.68 Co 2.10	6.80 2.12
[Fe _{0.69} Co _{0.31} (3-OCH ₃ -SalEen) ₂]PF ₆	44.84	44.80	5.29	5.22	8.71	8.58	Fe 5.99 Co 2.66	5.94 2.81
[Fe _{0.60} Co _{0.40} (3-OCH ₃ -SalEen) ₂]PF ₆	44.74	44.92	5.28	5.26	8.69	8.61	Fe 5.20 Co 3.66	5.23 3.59
[Fe _{0.50} Co _{0.50} (3-OCH ₃ -SalEen) ₂]PF ₆	44.72	44.64	5.27	5.32	8.61	8.73	Fe 4.33 Co 4.57	4.44 4.73
[Fe _{0.30} Co _{0.70} (3-OCH ₃ -SalEen) ₂]PF ₆	44.68	45.17	5.27	5.54	8.68	8.43	Fe 2.60 Co 6.39	2.90 6.00
[Fe _{0.79} Co _{0.21} (SalEen) ₂]PF ₆	45.27	44.99	5.14	5.26	9.59	9.31	Fe 7.52 Co 2.16	7.41 2.11
[Fe _{0.60} Co _{0.40} (SalEen) ₂]PF ₆	45.23	45.08	5.13	5.29	9.58	9.10	Fe 5.73 Co 4.03	5.91 3.95
[Fe _{0.36} Co _{0.64} (SalEen) ₂]PF ₆	45.17	45.40	5.13	5.37	9.57	9.41	Fe 3.44 Co 6.45	3.39 6.33
[Cr(3-OCH ₃ -SalEen) ₂]PF ₆	45.10	45.24	5.32	5.48	8.76	9.00	8.13	8.33
[Cr(SalEen) ₂]PF ₆	45.62	45.37	5.18	5.32	9.67	9.60	8.98	8.57
[Fe _{0.65} Cr _{0.35} (3-OCH ₃ -SalEen) ₂]PF ₆	44.92	45.61	5.30	5.22	8.73	9.07	Fe 5.65 Cr 2.84	5.45 2.75
[Fe _{0.50} Cr _{0.50} (3-OCH ₃ -SalEen) ₂]PF ₆	44.96	45.04	5.30	5.46	8.74	8.74	Fe 4.36 Cr 4.06	4.26 3.97
[Fe _{0.40} Cr _{0.60} (3-OCH ₃ -SalEen) ₂]PF ₆	44.99	45.25	5.31	5.39	8.74	9.02	Fe 3.49	3.51
[Fe _{0.50} Cr _{0.50} (SalEen) ₂]PF ₆	45.47	45.30	5.16	5.04	9.64	9.56	Fe 4.81 Cr 4.47	4.94 4.57
[Fe _{0.25} Cr _{0.75} (SalEen) ₂]PF ₆	45.55	45.28	5.17	5.22	9.65	9.86	Fe 2.41	2.45

a cooperative phase transition in the solid state. Small homogeneous regions (domains) of minority-spin molecules form in the crystallite of majority-spin molecules. There is kinetic control in the solid state. Before a minority-spin domain can persist and continue to grow, it has to attain a critical size. The critical size is generally believed to be temperature dependent. Kinetic control could result by virtue of the fact that the growth of a minority-spin domain involves the incorporation into the minority-spin domain of majority-spin molecules on the boundaries of the domain. If the boundary of the minority-spin domain encounters a defect in the crystal, then the activation energy for further growth of the minority-spin domain will be increased.^{3,4} Crystallites are rarely free of defects such as vacancies, crystal dislocations, and impurities. At the same time that the presence of crystal defects inhibits the growth of critical-size minority-spin domains, crystal defects are also preferred sites for the initial formation of minority-spin domains. This sensitivity to defects could explain why different preparations of a given compound can have different characteristics. Compounds that tend to solvate could be prone to have additional crystal defects which result from the loss of a small number of solvent molecules. It was the goal of the work described in this second paper to obtain evidence to substantiate the presence of the nucleation and growth mechanism. Defects were introduced into the microcrystalline [Fe(X-SalEen)₂]Y spin-crossover complexes by mechanically grinding the compounds and by doping them into isostructural cobalt(III) and chromium(III) hosts.

The effects of defects have been noted for other compounds involved in phase transitions. For example, the effect of compound grinding on the II-III phase transformation of hydrazinium(2+) sulfate was very recently reported.⁵ The transformation was monitored by differential thermal analysis

(DTA). It was observed that the DTA peak is sharpest and occurs at the highest temperature for the sample containing the largest crystallites. Grinding the sample to reduce the crystallite size made the DTA peak more diffuse and shifted it to lower temperatures.

Experimental Section

Physical Measurements. Variable-temperature magnetic susceptibility, EPR, and ⁵⁷Fe Mössbauer experiments were carried out as indicated in the preceding paper.

It is necessary to correct for the paramagnetic susceptibility of the host chromium(III) compound in order to evaluate the paramagnetic susceptibility of the iron(III) ions doped into the chromium compound. First, the molar paramagnetic susceptibility χ_M of [Cr(3-OCH₃-SalEen)₂]PF₆ was determined as a function of temperature and least-squares fit to the Curie-Weiss equation to give

$$\chi_M^{\text{Cr}} = (1.88/T) + 0.18$$

If χ_M^{Fe} is the molar paramagnetic susceptibility for the iron component in the doped compound [Fe_xCr_{1-x}(3-OCH₃-SalEen)₂]PF₆, then the measured molar paramagnetic susceptibility for the doped compound, χ_M , is given as

$$\chi_M = x\chi_M^{\text{Fe}} + (1-x)\chi_M^{\text{Cr}}$$

The cobalt(III) hosts are essentially diamagnetic; a correction for the TIP contribution of the host lattice would lead to a minimal change in the calculated μ_{eff} of a doped sample and was therefore deemed unnecessary.

X-ray powder patterns were obtained with a Norelco powder diffractometer employing a copper K α X-ray source.

Compound Preparation. Elemental analyses were performed in the Microanalytical Laboratory of the School of Chemical Sciences. Analytical data are collected in Table I.

[Co(3-OCH₃-SalEen)₂]NO₃. A methanol solution (30 mL) of 1.76 g of *N*-ethylethylenediamine was added to a 30-mL methanol solution of 3.04 g of 3-methoxysalicylaldehyde to give a yellow solution of the Schiff base. An aqueous solution (5 mL) of 0.84 g of NaOH was added, followed by the slow addition of 40 mL of methanol containing 4.0 g of Co(NO₃)₂·6H₂O. A dark brown precipitate formed almost immediately upon addition of the cobalt(II) nitrate solution. The

(4) Christian J. W. "The Theory of Transformations in Metals and Alloys", 2nd ed.; Pergamon Press: Oxford, 1975; Part I.

(5) Okamoto, T.; Nakamura, N.; Chihara, H. *Bull. Chem. Soc. Jpn.* **1979**, *52*, 1619.

solution was stirred and heated to boiling during all of the additions. Oxidation to give the cobalt(III) complex was carried out either by adding 50 mL of 3% H_2O_2 aqueous solution or by adding 3 mL of 30% H_2O_2 solution. Care should be exercised when adding H_2O_2 to avoid overflowing the solution. After the oxidant was added, the solution was boiled for an additional 5 min. The desired compound precipitated at this point and was filtered, washed with water and ether, and then dried in vacuo over P_2O_{10} . On occasion it was necessary to stir the product in a minimum amount of H_2O to remove some NaNO_3 . Samples of $[\text{Co}(\text{SalEen})_2]\text{NO}_3$ were prepared with the same procedure. The compound $[\text{Co}(\text{SalEen})_2]\text{NO}_3$ does not precipitate as rapidly as the 3-methoxy analogue. It is necessary to cool the hot solution.

$[\text{Co}(3\text{-OCH}_3\text{-SalEen})_2]\text{PF}_6$ and $[\text{Co}(\text{SalEen})_2]\text{PF}_6$. Microcrystalline samples of these compounds were prepared by metathesis of the corresponding NO_3^- salts in CH_3OH with NaPF_6 .

$[\text{Cr}(3\text{-OCH}_3\text{-SalEen})_2]\text{PF}_6$. This compound was prepared by the metathesis of $[\text{Cr}(3\text{-OCH}_3\text{-SalEen})_2]\text{Cl}$, which was prepared in the following way. A strong stream of N_2 was passed through a 70-mL methanol solution of 3.04 g of 3-methoxysalicylaldehyde, 1.76 g of *N*-ethylethylenediamine, and 0.084 g of NaOH . A stoichiometric or less than stoichiometric amount (ca. 1.10 g) of anhydrous CrCl_2 was weighed under a nitrogen atmosphere and then quickly added to the solution. Almost immediately a brown-yellow product precipitated. To ensure complete oxidation to chromium(II), 3 mL of 30% H_2O_2 solution was introduced, followed by boiling for 5 min. The product obtained was found to be pure enough to carry out the metathesis with NaPF_6 in absolute methanol. The compound $[\text{Cr}(\text{SalEen})_2]\text{PF}_6$ was also formed by metathesis of the corresponding chloride salt.

$[\text{Fe}_x\text{M}_{1-x}(3\text{-OCH}_3\text{-SalEen})_2]\text{PF}_6$. The cobalt(III)- and chromium(III)-doped compounds were prepared by dissolving either $[\text{Co}(3\text{-OCH}_3\text{-SalEen})_2]\text{PF}_6$ or $[\text{Cr}(3\text{-OCH}_3\text{-SalEen})_2]\text{PF}_6$ together with $[\text{Fe}(3\text{-OCH}_3\text{-SalEen})_2]\text{PF}_6$ in the desired ratio in boiling absolute methanol. The doped compound was obtained by cooling of the solution in a refrigerator. Typically, the total weight used was 0.50 g, and the volume of the methanol solution was kept to 50 mL. The doped $[\text{Fe}_x\text{M}_{1-x}(\text{SalEen})_2]\text{PF}_6$ compounds were prepared in the same manner.

Results and Discussion

Hysteresis. König and co-workers⁶ have recently shown that the investigation of hysteresis effects associated with almost discontinuous spin-crossover transitions can be useful to understand the mechanism of such transitions. They studied the $^5\text{T}_2$ to $^1\text{A}_1$ transition in $\text{Fe}(\text{bt})_2(\text{NCS})_2$, where bt is 2,2'-bi-2-thiazoline, and found a hysteresis of 9.5 K. An independent-domain model was used to fit the temperature-dependent ^{57}Fe Mössbauer and X-ray powder diffraction data.

The compound $[\text{Fe}(3\text{-OCH}_3\text{-SalEen})_2]\text{PF}_6$ is an iron(III) compound that shows an almost discontinuous spin-crossover transition, as indicated in the preceding paper. A 50-mCi source of ^{57}Co in rhodium was used to obtain Mössbauer spectra. The compound was first cooled to 87 K, and a spectrum was taken. Table II gives the data. The sample was then warmed to room temperature, and spectra were recorded at several temperatures along the way. Some of the spectra obtained in the region of the spin-crossover transition, each of which took ca. 5 h to accumulate, are illustrated in Figure 1. After the warming cycle was completed, the sample was cooled, and four spectra were recorded in the transition region. Two facts are evident from an examination of Figure 1. There is a hysteresis of 2–4° in $[\text{Fe}(3\text{-OCH}_3\text{-SalEen})_2]\text{PF}_6$. It would be necessary to shorten the time required to run each spectrum and make more detailed measurements in order to characterize the hysteresis more completely. However, it is clear from the data in Table II and Figure 1 that in the temperature region where the spin-crossover occurs in $[\text{Fe}(3\text{-OCH}_2\text{-SalEen})_2]\text{PF}_6$ only two electronic states are present.

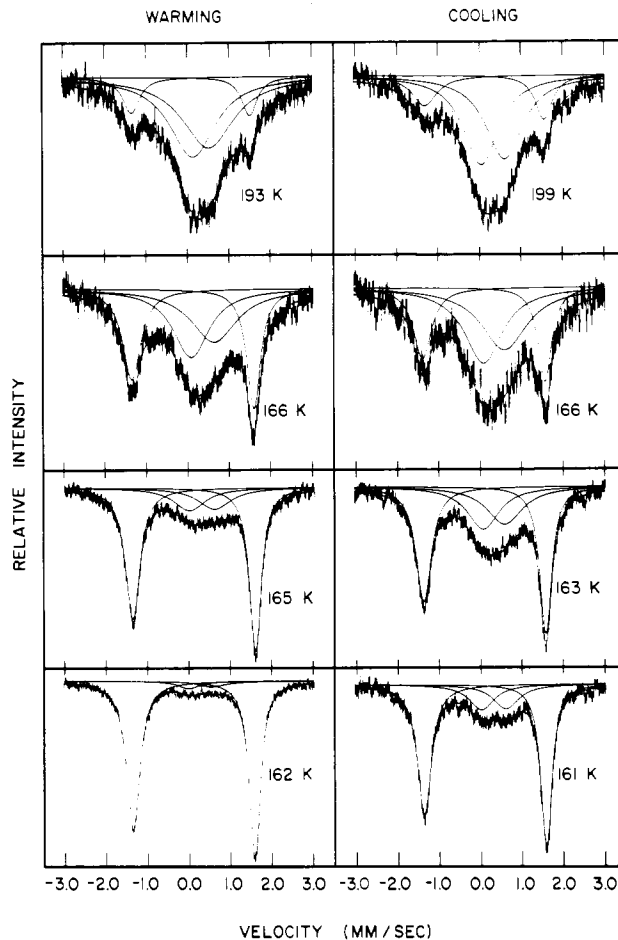


Figure 1. Temperature variation of the ^{57}Fe Mössbauer spectrum for $[\text{Fe}(3\text{-OCH}_3\text{-SalEen})_2]\text{PF}_6$. The sample was first cooled to 87 K, and then spectra were recorded as the sample temperature was increased. Then spectra were obtained as the sample was cooled again.

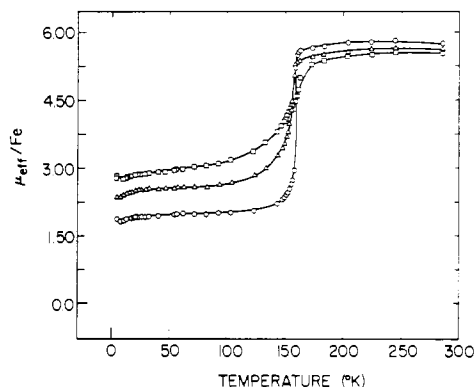


Figure 2. Effective magnetic moment per iron ion ($\mu_{\text{eff}}/\text{Fe}$) vs. temperature curve for $[\text{Fe}(3\text{-OCH}_3\text{-SalEen})_2]\text{PF}_6$: O, unperturbed microcrystalline solid; Δ , same solid ground with mortar and pestle; \square , same solid ground in a ball mill.

Effect of Grinding Complexes. As recently communicated,⁷ we have found that grinding the $[\text{Fe}(\text{X-SalEen})_2]\text{Y}$ spin-crossover complexes affects the properties of these compounds. One microcrystalline sample of $[\text{Fe}(3\text{-OCH}_3\text{-SalEen})_2]\text{PF}_6$ (preparation 1) was divided into three parts. One part was left unperturbed, while another was ground with a mortar and pestle. The third fraction was more thoroughly ground in a ball mill for a period of 30 min. Magnetic susceptibilities were

(6) König, E.; Ritter, G.; Irlner, W.; Nelson, S. M. *Inorg. Chim. Acta* 1979, 37, 169 and references therein.

(7) Haddad, M. S.; Federer, W. D.; Lynch, M. W.; Hendrickson, D. N. *J. Am. Chem. Soc.* 1980, 102, 1468.

Table II. Iron-57 Mössbauer Fitting Parameters for $[\text{Fe}(\text{3-OCH}_3\text{-SalEen})_2]\text{PF}_6$

T, K^b	$\delta, \text{mm s}^{-1 a, b}$	$\Delta E_Q, \text{mm s}^{-1 b}$	$\Gamma, \text{mm s}^{-1 b, c}$	% area ^b
Warming Sample				
87 (1)	+0.235 (1)	2.843 (2)	0.172 (2), 0.147 (2)	100
113 (1)	+0.227 (4)	2.835 (8)	0.19 (1), 0.147 (7)	100
122 (1)	+0.239 (1)	3.004 (1)	0.187 (2), 0.157 (1)	100
131 (1)	+0.223 (3)	2.826 (6)	0.192 (7), 0.155 (5)	100
153 (1)	+0.34 (5)	0.62 (6)	0.28 (6), 0.30 (7)	4.6 (1)
	+0.229 (1)	2.993 (2)	0.198 (2), 0.163 (1)	95.4 (9)
158.5 (0.5)	+0.21 (4)	0.64 (8)	0.23 (5), 0.37 (10)	5.0 (1)
	+0.227 (1)	2.974 (2)	0.194 (2), 0.162 (2)	95.0 (1.0)
162.5 (0.5)	+0.38 (3)	0.55 (6)	0.31 (6), 0.41 (9)	7.4 (1)
	+0.226 (1)	2.939 (2)	0.192 (2), 0.160 (1)	92.6 (1.0)
165 (0.5)	+0.43 (2)	0.60 (4)	0.46 (5), 0.49 (6)	27.6 (5)
	+0.224 (2)	2.958 (3)	0.210 (4), 0.168 (3)	72.4 (1.2)
166.5 (0.5)	+0.28 (2)	0.55 (5)	0.52 (4), 0.67 (8)	59.8 (1.7)
	+0.23 (1)	2.93 (1)	0.27 (1), 0.20 (1)	40.2 (1.2)
168 (0.5)	+0.46 (2)	0.54 (5)	0.56 (4), 0.72 (8)	69.6 (2.2)
	+0.22 (1)	2.90 (1)	0.28 (2), 0.20 (1)	30.4 (1.0)
170 (0.5)	+0.43 (2)	0.48 (4)	0.51 (3), 0.58 (5)	67.6 (1.4)
	+0.23 (1)	2.88 (1)	0.29 (2), 0.22 (1)	32.4 (6)
173 (0.5)	+0.40 (4)	0.42 (10)	0.72 (8), 0.65 (6)	75.0 (2.5)
	+0.21 (1)	2.91 (2)	0.30 (2), 0.22 (2)	25.0 (8)
193 (1) ^{d, f}	+0.43 (5)	0.38 (14)	0.67 (6), 0.75 (11)	86.0 (4.1)
	+0.20 (2)	2.84 (3)	0.24 (4), 0.22 (3)	14.0 (6)
193 (1) ^{e, f}	+0.42 (2)	0.53 (3)	0.51 (3), 0.54 (3)	75.0
	+0.21 (2)	2.79 (3)	0.38 (3), 0.33 (2)	25.0
293 (2) ^g	+0.45 (5)	0.35 (14)	1.08 (18), 0.70 (4)	100
Cooling Sample				
161 (0.5)	+0.43 (2)	0.59 (3)	0.37 (4), 0.39 (4)	26.6 (5)
	+0.226 (2)	2.940 (4)	0.200 (4), 0.160 (3)	73.4 (1.3)
163.5 (0.7)	+0.45 (2)	0.52 (4)	0.47 (4), 0.53 (5)	43.8 (9)
	+0.226 (3)	2.928 (5)	0.223 (6), 0.174 (5)	56.2 (1.2)
166.5 (0.7)	+0.47 (4)	0.51 (8)	0.56 (6), 0.68 (11)	69.2 (3.0)
	+0.22 (1)	2.94 (2)	0.26 (2), 0.20 (2)	30.8 (1.3)
199 (1)	+0.44 (1)	0.56 (3)	0.51 (3), 0.55 (4)	80.6 (2.2)
	+0.24 (2)	2.86 (4)	0.37 (5), 0.25 (3)	19.4 (5)

^a Isomer shifts are relative to Fe metal. ^b Error in last significant figure is given in parentheses. ^c Half-width at half-maximum listed in order of increasing velocity of the peak. ^d Relative areas of low-spin and high-spin doublets were varied. ^e Relative areas of low-spin and high-spin doublets were fixed in fitting. ^f The two different fits obtained for the 193 K spectrum gave virtually identical goodness of fit parameters but significantly different Mössbauer parameters. This suggests that, when substantial portions of both spin states are present, systematic errors in the division of the total area between the two doublets may be introduced. ^g We were unable to obtain a reasonable four-line fit for this broad spectrum even though weak shoulders due to a low-spin doublet are clearly evident.

determined for the three samples from 286 to 4.2 K; plots of $\mu_{\text{eff}}/\text{Fe}$ vs. temperature are given in Figure 2, and the data are given in Tables III-V.⁸ Grinding a sample can be seen to affect dramatically the nature of the spin-crossover transition. A comparison of the $\mu_{\text{eff}}/\text{Fe}$ vs. temperature curves for the two ground samples with that obtained for the unperturbed sample shows that there are four effects of grinding that can be listed: (1) Grinding leads to an incompleteness of the transition. (2) The transition becomes more gradual. (3) There is a formation of more low-spin molecules in the ground samples at higher temperatures. (4) The temperature at which there are equal numbers of low-spin and high-spin molecules shifts to a lower value upon sample grinding.

The two $[\text{Fe}(\text{3-OCH}_3\text{-SalEen})_2]\text{PF}_6$ samples that were ground show a plateau in their $\mu_{\text{eff}}/\text{Fe}$ vs. temperature curves below ca. 100 K. In the case of the sample ground in the ball mill this plateau occurs at a $\mu_{\text{eff}}/\text{Fe}$ value of $2.8 \mu_B$. The unperturbed sample has $\mu_{\text{eff}}/\text{Fe} = 1.83 \mu_B$ at 4.2 K. The latter value is characteristic of a low-spin ferric complex. In the case of a ground compound, thus, it appears that a certain fraction of the molecules persists in the high-spin state.

The above effects of grinding were found to be reproducible. A portion of the microcrystalline preparation 3 of $[\text{Fe}(\text{3-OCH}_3\text{-SalEen})_2]\text{PF}_6$ was ground in a ball mill for approximately 30 min. Magnetic susceptibility data are given in Table

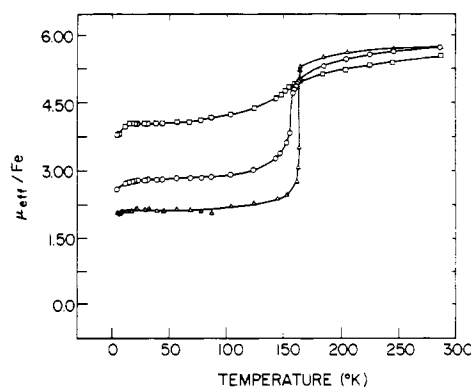


Figure 3. Effective magnetic moment per iron ion ($\mu_{\text{eff}}/\text{Fe}$) vs. temperature curves for an apparently noncrystalline sample of $[\text{Fe}(\text{3-OCH}_3\text{-SalEen})_2]\text{PF}_6$: O, unperturbed powder; □, same powder ground in a ball mill; Δ, ground sample recrystallized by evaporating a methanol solution to dryness.

VI.⁸ There is a plateau at $3.2 \mu_B$, whereas an unperturbed fraction of this same preparation 3 was found to undergo a complete transition.

In the preceding paper the preparation and properties of a powdered sample (preparation 2) of $[\text{Fe}(\text{3-OCH}_3\text{-SalEen})_2]\text{PF}_6$ were described. This material was intentionally precipitated from solution very rapidly and to the eye appeared not to be microcrystalline. It was of interest to see how this

(8) Supplementary material.

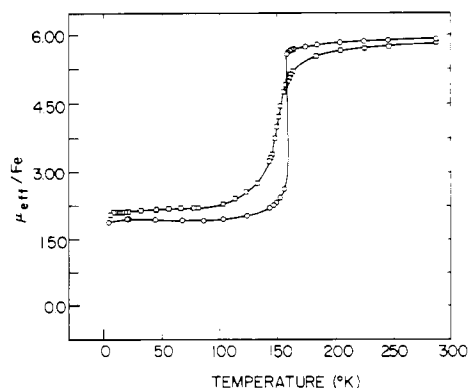


Figure 4. Effective magnetic moment per iron ion ($\mu_{\text{eff}}/\text{Fe}$) vs. temperature for $[\text{Fe}(\text{3-OCH}_3\text{-SalEen})_2]\text{PF}_6$: \circ , unperturbed microcrystalline solid; \square , same solid subjected to pressure.

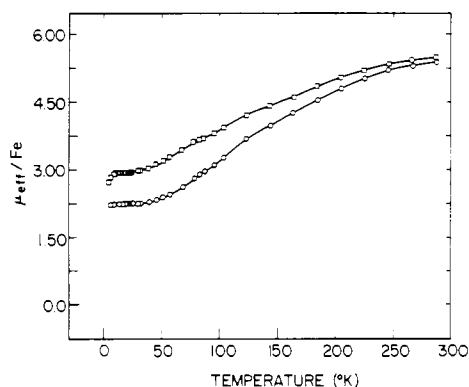


Figure 5. Effective magnetic moment per iron ion ($\mu_{\text{eff}}/\text{Fe}$) vs. temperature for $[\text{Fe}(\text{SalEen})_2]\text{PF}_6$: \circ , unperturbed microcrystalline sample; \square , same solid ground in a ball mill.

sample would respond to grinding. The magnetic susceptibility data for the unperturbed powder are given in the preceding paper, where it was found that there is a low-temperature plateau at $\mu_{\text{eff}}/\text{Fe} = 3.0 \mu_B$. A portion of this sample was ground in a ball mill for 30 min. Figure 3 shows that grinding this material makes the transition even more gradual, and the plateau now occurs at a value of $\mu_{\text{eff}}/\text{Fe} = 4.0 \mu_B$ (see Table VII⁸ for the data). For elimination of the possibility that grinding leads to compound decomposition and that this explains the observations, the ground sample of preparation 2 was dissolved in absolute methanol, and then the solution was evaporated to dryness to give a microcrystalline solid. Evaporating the solvent to dryness would retain any impurity. In Figure 3 (and Table VIII⁸) it can be seen that this recrystallized sample shows a sudden and complete phase transition as noted for preparations 1 and 3 of $[\text{Fe}(\text{3-OCH}_3\text{-SalEen})_2]\text{PF}_6$.

In another experiment it was found that the application of pressure to a microcrystalline sample of $[\text{Fe}(\text{3-OCH}_3\text{-SalEen})_2]\text{PF}_6$ affects the spin-crossover transition. A microcrystalline sample of the compound (preparation 4) was loaded into a 13-mm die used to prepare KBr disks for IR spectroscopy. The sample was then subjected to some 20 000 lb of pressure for 5 min. Figure 4 and Table IX⁸ show that this treatment leads to the same four effects that were seen for sample grinding.

Similar effects were observed when a sample of $[\text{Fe}(\text{SalEen})_2]\text{PF}_6$ was ground. As a microcrystalline solid, this compound undergoes a gradual, but complete, spin-crossover transition. Figure 5 (see Table X⁸) shows the $\mu_{\text{eff}}/\text{Fe}$ vs. temperature curves for an unperturbed sample and for a sample ground in a ball mill. Again grinding results in an incompleteness of the transition where in this case there is a

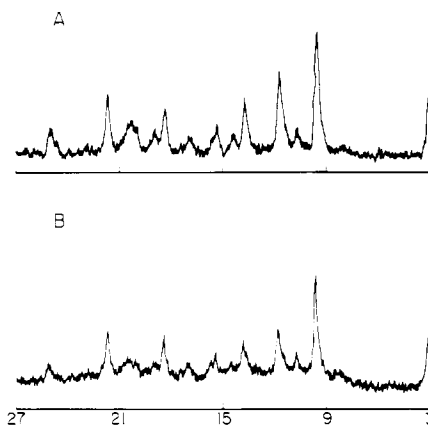


Figure 6. X-ray powder diffraction patterns of $[\text{Fe}(\text{3-OCH}_3\text{-SalEen})_2]\text{PF}_6$: A, unperturbed, microcrystalline sample; B, same solid ground in a ball mill. A scan rate of 1° of $2\theta/\text{min}$ was employed.

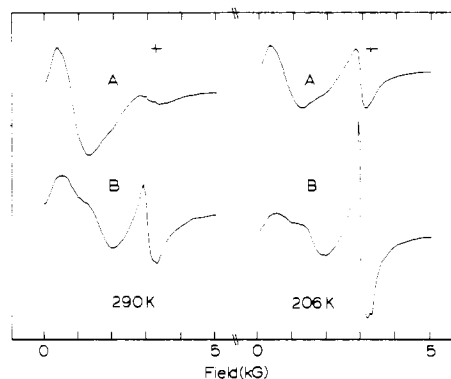


Figure 7. X-Band EPR spectra of $[\text{Fe}(\text{3-OCH}_3\text{-SalEen})_2]\text{PF}_6$ at 290 and 206 K: A, unperturbed microcrystalline solid; B, same solid ground in a ball mill.

plateau at $\mu_{\text{eff}}/\text{Fe} = 2.9 \mu_B$ in the 10–30 K range. The transition is also more gradual compared to that for the unperturbed compound.

Several physical techniques were used to show that compound grinding does not result in a structural change and that the same two electronic states are present that were found for the unperturbed compounds. The room-temperature X-ray powder diffraction patterns, shown in Figure 6, of the unground sample and a sample of $[\text{Fe}(\text{3-OCH}_3\text{-SalEen})_2]\text{PF}_6$ (preparation 1) ground in a ball mill are essentially identical. It is clear that no structural changes occurred and that, if there were any sample decomposition, then the decomposition product does not diffract.

X-Band EPR spectra were recorded for unperturbed microcrystalline and ground samples of $[\text{Fe}(\text{3-OCH}_3\text{-SalEen})_2]\text{PF}_6$ between room temperature and liquid-nitrogen temperature. The spectral features were found to be the same for the unperturbed and ground samples, except for the relative intensities of the signals. At room temperature, the low-spin ($g \approx 2$) signal for the ground samples has an increased relative intensity in keeping with the values of $\mu_{\text{eff}}/\text{Fe}$ for the ground samples at room temperature which are smaller than those for unperturbed sample. Thus, there is a greater percentage of molecules in the low-spin state at room temperature as a result of sample grinding. In addition, whereas the unperturbed sample shows no high-spin signal at 77 K, the ground samples show a high-spin signal ($g \approx 4.3$) at 77 K, in keeping with the plateaus in the $\mu_{\text{eff}}/\text{Fe}$ vs. temperature curves. This $g \approx 4.3$ signal is due to those high-spin molecules that have somehow resisted the conversion to low spin. It is intriguing, in fact, that this high-spin signal occurs at $g \approx 4.3$. Figure 7 illustrates the differences in spectra between an unperturbed

Table XI. Iron-57 Mössbauer Fitting Parameters for Machine-Ground $[\text{Fe}(\text{3-OCH}_3\text{-SalEen})_2]\text{PF}_6^a$

T, K	δ , mm $s^{-1} b, c$	ΔE_Q , mm $s^{-1} c$	Γ , mm $s^{-1} c, d$	% area
293 (2)	+0.38 (2)	0.60 (3)	0.37 (4), 0.42 (5)	57.4 (3.4)
	+0.27 (9)	2.30 (23) ^f	0.77 (17), 0.77 (14)	42.6 (2.5)
245 (2)	+0.35 (7)	0.31 (18)	0.79 (14), 0.70 (6)	82.0 (3.6)
	+0.19 (2)	2.71 (4) ^f	0.43 (6), 0.40 (5)	18.0 (8)
215 (2)	+0.40 (1)	0.56 (2)	0.54 (2), 0.54 (2)	79.4 (1.2)
	+0.19 (1)	2.75 (2)	0.30 (2), 0.27 (2)	20.6 (4)
185 (0.5)	+0.42 (8)	0.18 (20)	0.70 (5), 0.90 (22)	80.2 (4.0)
	+0.20 (1)	2.74 (1)	0.26 (2), 0.20 (1)	19.8 (1.0)
172 (1)	+0.42 (7)	0.23 (18)	0.68 (4), 0.93 (25)	73.6 (4.2)
	+0.20 (1)	2.77 (1)	0.27 (2), 0.20 (1)	26.4 (1.5)
163 (1)	+0.50 (3)	0.50 (7)	0.54 (5), 0.77 (13)	73.8 (2.6)
	+0.21 (1)	2.78 (1)	0.26 (2), 0.19 (1)	36.2 (1.5)
152 (1)	+0.42 (3)	0.59 (5)	0.48 (5), 0.57 (8)	44.0 (1.2)
	+0.22 (3)	2.832 (7)	0.23 (1), 0.166 (6)	56.0 (1.4)
143 (2)	+0.31 (5)	0.66 (8)	0.36 (8), 0.46 (12)	37.0 (2.0)
	+0.44 (1)	2.84 (2)	0.22 (2), 0.17 (1)	63.0 (3.6)
131 (0.5)	+0.39 (21) ^e	^e	^e	41.8 (31.1)
	+0.219 (2)	2.833 (5)	0.20 (1), 0.16 (1)	58.2 (43.2)
114 (1)	^e	^e	^e	31.2 (2.0)
	+0.233 (2)	2.852 (2)	0.203 (6), 0.156 (2)	68.8 (4.6)
90 (2)	^e	^e	^e	22.8 (1.4)
	+0.238 (1)	2.871 (2)	0.200 (2), 0.157 (2)	77.2 (4.6)

^a At each temperature the upper row represents the data for the high-spin doublet and the lower row represents the data for the low-spin doublet. ^b Isomer shifts relative to Fe metal. ^c Error in last significant figure is given in parentheses. ^d Half-width at half-maximum listed in order of increasing velocity of the peak. ^e No meaningful parameters could be obtained for the broad and weak components of the inner doublet due to poor resolution. ^f We believe that the marked decrease in the calculated ΔE_Q value at high temperature is not real but rather is caused by one or both of two reasons: (1) systematic errors in the fitting procedure are as described in Table II, footnote f; (2) increased spin-flipping rates at high temperatures may be nearly as fast as the reciprocal of the Mössbauer time scale.

sample (A) and a sample ground in a ball mill (B). As indicated in the preceding paper, the sudden transition system $[\text{Fe}(\text{3-OCH}_3\text{-SalEen})_2]\text{PF}_6$ has its high-spin signal at $g \approx 7.5$, in contrast to the other molecules which show $g \approx 4.3$ signals. Figure 7 shows that grinding this sudden system leads to the appearance of a new signal at $g \approx 4.3$. This new high-spin signal does not disappear when the ground sample is cooled to 77 K. It is known that EPR signals for high-spin ferric complexes are very sensitive to strains in the crystal.⁹ Zero-field splitting in the high-spin state is gauged by $\hat{H} = D\hat{S}_z^2 + E(\hat{S}_x^2 - \hat{S}_y^2)$, where D and E are the axial and rhombic zero-field splitting parameters, respectively. A complex with rhombic symmetry exhibits an intense $g \approx 4.3$ signal if $E/D \approx 1/3$ and $h\nu/D \leq 3$. A shift to larger g values could mean that the complex has a more nearly axial symmetry with $E \approx 0$. It would be interesting to know whether the molecules giving the $g \approx 4.3$ signal in the ground $[\text{Fe}(\text{3-OCH}_3\text{-SalEen})_2]\text{PF}_6$ sample are located on the surface of the crystallites or distributed throughout the crystallites.

Mössbauer spectra were run for a sample of $[\text{Fe}(\text{3-OCH}_3\text{-SalEen})_2]\text{PF}_6$ ground in a ball mill (see Table XI). Figure 8 shows that the spectra support the conclusions obtained from the other techniques, namely, that only signals from two electronic states can be seen for the ground sample. It can be seen that the relative amounts of high-spin and low-spin signals are changed at a given temperature, when compared to the unperturbed sample.

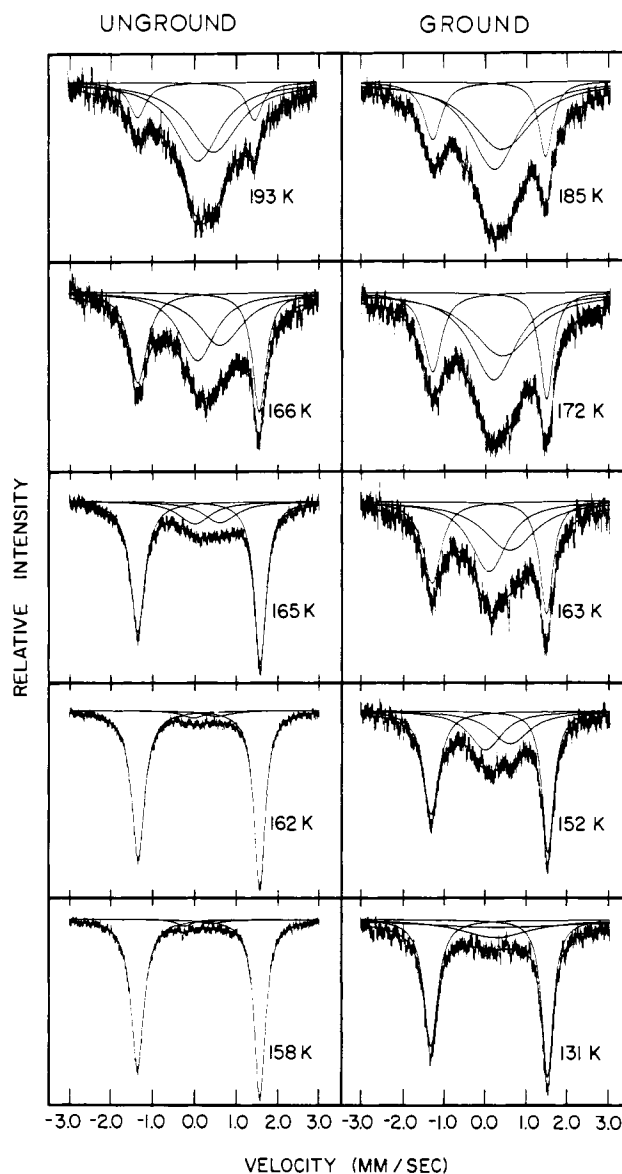


Figure 8. Temperature variation of ^{57}Fe Mössbauer spectrum for $[\text{Fe}(\text{3-OCH}_3\text{-SalEen})_2]\text{PF}_6$. The same microcrystalline sample that was examined in the hysteresis run was ground in a ball mill, and spectra were recorded at various temperatures.

The above observations on ground samples of spin-crossover complexes are explicable in terms of the nucleation and growth mechanism of phase transitions in solids.^{3,4} Three aspects of this mechanism are reflected in our data: (a) defects such as crystal imperfections, impurities, and dislocations are preferred nucleation sites; (b) the greater is the number of defects, the greater is the possibility that a growth site will collide with another site or a crystal dislocation and this will increase the activation barrier for the growth process and slow the transformation; (c) there is a direct proportionality between the critical size required for the minority domain to persist and the absolute temperature, and, as a consequence, fewer critical-sized minority domains form at higher temperatures than do at lower temperatures.

Grinding a spin-crossover complex would be expected to increase the number of crystal defects. It is not possible, of course, to see these defects directly. Possible defect structure could include fissures, cracks, or irregular features that develop on the surface of the microcrystallites upon grinding. Other possible defects could be internal in the microcrystallites such as dislocations where there is slippage of some unit cells relative to the remainder of the crystal.

(9) (a) Stevens, K. W. H. *Proc. R. Soc. London, Ser. A* 1953, 542. (b) Griffith, J. S. "The Theory of Transition Metal Ions"; Cambridge University Press: London, 1961; p 364. (c) Ayscough, P. B. "Electron Spin Resonance in Chemistry"; Methuen: London, 1967; p 117.

Microcrystals of $[\text{Fe}(\text{3-OCH}_3\text{-SalEen})_2]\text{PF}_6$ were suspended in water and examined with an optical microscope at a magnification of 3200. The unground microcrystals appeared as parallelepipeds, which for the most part are transparent. Grinding these same microcrystals in a ball mill for 30 min reduced the average crystal size by a factor of 50. In the water suspension, a good percentage of the ground crystallites tended to cluster. It was not readily possible to examine the surface of one of the small crystallites resulting from the grinding.

If it is accepted that grinding does increase the defect structure in the microcrystals of the ferric spin-crossover complex, it then follows from the tenets of the nucleation and growth mechanism that there will be a greater concentration of nucleation sites in the ground sample than in the unground sample. This explains one of our observations, namely, that grinding leads to the formation of more low-spin molecules at high temperatures, because defects are preferred sites for nucleation of a low-spin domain. In Figure 2, for example, it can be seen that, compared to the unground and mortar and pestle ground samples, the sample of $[\text{Fe}(\text{3-OCH}_3\text{-SalEen})_2]\text{PF}_6$ which was ground in a ball mill has the smallest $\mu_{\text{eff}}/\text{Fe}$ at 286 K.

It is also possible to explain why grinding a ferric spin-crossover complex makes the transition more gradual and shifts the temperature at which the transition occurs to a lower value. The growth of the low-spin domains, homogeneous regions where all the molecules are in the lowest energy Kramers doublet, is rate determining in the nucleation and growth mechanism. There is kinetic control. If the boundary of a low-spin domain impinges upon a defect as it grows or contacts another low-spin domain, the activation barrier for the growth process will be increased. The concentration of defects is greater in the ground sample compared to the unperturbed sample, and, consequently, the activation energy for the growth of low-spin domains is greater in the ground sample. This shifts the transition to a lower temperature and makes the transition more gradual.

The tendency to exhibit an incomplete spin-crossover transition, as reflected by a plateau in the $\mu_{\text{eff}}/\text{Fe}$ vs. temperature at a value intermediate between low spin and high spin, is also due to the increased activation for growth of low-spin domains in the ground samples. The growth is slowed down to such a slow rate that, as the sample temperature is further decreased, there is very little change in relative amounts of low-spin and high-spin complexes. In the preceding paper we did, in fact, point out two cases^{10,11} of spin-crossover complexes that were quenched to a low temperature, and the rate at which the complex approached an equilibrium value was monitored.

The loss of the suddenness of the transition in $[\text{Fe}(\text{3-OCH}_3\text{-SalEen})_2]\text{PF}_6$ upon grinding and the shift of the transition drop to a lower temperature could be explained by the phenomenological model used by Sorai et al.¹² and Gütllich et al.¹³ In their work almost discontinuous spin-crossover transitions were observed for ferrous complexes. Domains of a new phase (low spin) formed in the domains of the old phase (high spin). A cooperativity was suggested whereupon a cooperativity enthalpy, $\Delta H^\circ_{\text{coop}}$, among ferrous complexes within a domain of the old phase was taken as the driving force. The larger the domain, the larger $\Delta H^\circ_{\text{coop}}$ is and the more sudden the transition becomes. It could be suggested that grinding a spin-crossover complex leads to smaller domains, and this makes the transition more gradual. The troubling point,

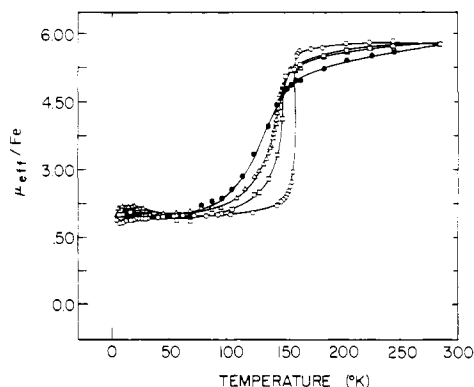


Figure 9. Effective magnetic moment per iron ion ($\mu_{\text{eff}}/\text{Fe}$) vs. temperature curves for microcrystalline $[\text{Fe}_x\text{Cr}_{1-x}(\text{3-OCH}_3\text{-SalEen})_2]\text{PF}_6$; O, $x = 1$; □, $x = 0.65$; △, $x = 0.50$; ●, $x = 0.40$.

however, is that the phenomenological model does not account for incomplete transitions where there are plateaus in the $\mu_{\text{eff}}/\text{Fe}$ vs. temperature curves. Whereas domain size ($\Delta H^\circ_{\text{coop}}$) is probably a factor, we believe that this factor alone is not sufficient.

Effect of Doping Complexes. Introducing metal ions other than iron(III) into the crystals of $[\text{Fe}(\text{X-SalEen})_2]\text{Y}$ spin-crossover complexes is, in effect, another way of introducing defects. We found it possible to prepare isostructural chromium(III) and cobalt(III) complexes with the compositions $[\text{M}(\text{3-OCH}_3\text{-SalEen})_2]\text{PF}_6$ and $[\text{M}(\text{SalEen})_2]\text{PF}_6$. These complexes do not, of course, undergo a spin-crossover transition.

Crystalline doped samples $[\text{Fe}_x\text{Cr}_{1-x}(\text{3-OCH}_3\text{-SalEen})_2]\text{PF}_6$ with $x = 0.65, 0.50,$ and 0.40 were prepared. Magnetic susceptibility data from 286 to 4.2 K were collected for $[\text{Cr}(\text{3-OCH}_3\text{-SalEen})_2]\text{PF}_6$. The data are given in Table XII,⁸ where it can be seen that $\mu_{\text{eff}}/\text{Cr} = 3.85 \mu_B$ at 286 K and that there is no sign of an appreciable intermolecular magnetic exchange interaction. These data were used (see Experimental Section) to calculate for a doped compound the fraction of the observed paramagnetism which is due to the iron(III) complexes. Magnetic susceptibility data for the three doped samples are collected in Tables XIII–XV.⁸ Figure 9 illustrates the variation with temperature of $\mu_{\text{eff}}/\text{Fe}$ for $[\text{Fe}(\text{3-OCH}_3\text{-SalEen})_2]\text{PF}_6$ and for the three doped samples. Inspection of the figure shows that, as the chromium(III) concentration is increased, the sharpness of the transition decreases and the transition temperature shifts to lower temperature.

It appears that the effects of doping are similar to some of the effects of grinding the sample, an expectation of the nucleation and growth mechanism of phase transitions in the solid state. A nucleus of low-spin complexes forms in a crystallite of high-spin complexes, and it grows into a critical-size low-spin domain. The rate-determining step for the overall transformation is the further growth of the low-spin domain, which occurs by the process of converting high-spin complexes into low-spin complexes at the boundary of the low-spin domain. In a doped sample, as a given low-spin domain grows, it can encounter a chromium(III) complex at the domain boundary. The activation barrier for the movement of the domain boundary is increased by such an encounter, as in the case of an encounter with a crystal defect caused by sample grinding. It is, thus, understandable why the spin-crossover phase transition becomes more gradual as the concentration of chromium(III) host is increased.

Gütllich et al.¹³ studied ferrous spin-crossover complexes doped into diamagnetic zinc(II) hosts. They also found that, as the concentration of host complexes was increased, the transition became more gradual, which was explained by suggesting the size of low-spin domains decreased as the

(10) Ritter, G.; König, E.; Irlner, W.; Goodwin, H. A. *Inorg. Chem.* **1978**, *17*, 224.

(11) Goodwin, H. A.; Smith, F. E. *Inorg. Nucl. Chem. Lett.* **1974**, *10*, 99.

(12) Sorai, M.; Seki, S. *J. Phys. Chem. Solids* **1974**, *35*, 555.

(13) Gütllich, P.; Köppen, H.; Link, R.; Steinhäuser, H. G. *J. Chem. Phys.* **1979**, *70*, 3977.

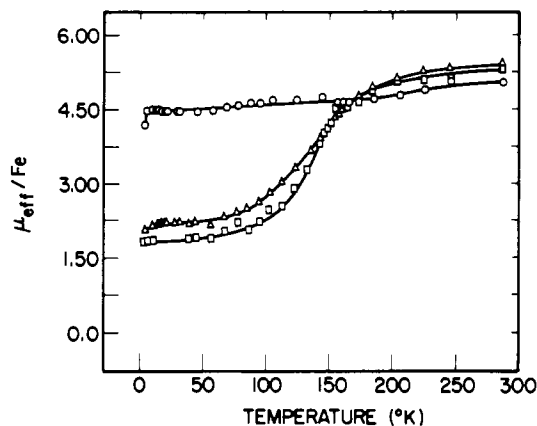


Figure 10. Effective magnetic moment per iron ion ($\mu_{\text{eff}}/\text{Fe}$) vs. temperature curves for $[\text{Fe}_{0.50}\text{Cr}_{0.50}(3\text{-OCH}_3\text{-SalEen})_2]\text{PF}_6$: Δ , unperturbed microcrystalline sample; O , same solid ground in a ball mill; \square , ground sample recrystallized by evaporating a methanol solution to dryness.

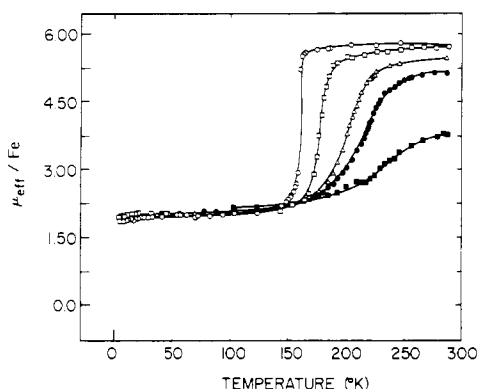


Figure 11. Effective magnetic moment per iron ion ($\mu_{\text{eff}}/\text{Fe}$) vs. temperature for microcrystalline $[\text{Fe}_x\text{Co}_{1-x}(3\text{-OCH}_3\text{-SalEen})_2]\text{PF}_6$: O , $x = 1$; \square , $x = 0.77$; Δ , $x = 0.69$; \bullet , $x = 0.60$; \blacksquare , $x = 0.50$.

concentration of host complexes was increased.

As an outgrowth of the idea that sample grinding and doping might be similarly affecting the spin-crossover transition, the effect of grinding a doped sample was explored. Figure 10 and Tables XVI–XVII⁸ show that the effect is dramatic. The crystalline sample of $[\text{Fe}_{0.5}\text{Cr}_{0.5}(3\text{-OCH}_3\text{-SalEen})_2]\text{PF}_6$ was ground in a ball mill for 30 min, and magnetic susceptibility data were collected. This same ground sample was then recrystallized by evaporating a methanol solution to dryness, and magnetic susceptibility data were recollected. Figure 10 shows that the unperturbed crystalline sample undergoes a gradual and essentially complete transition. The ground sample starts with $\mu_{\text{eff}}/\text{Fe} = \text{ca. } 5.0 \mu_{\text{B}}$ at 286 K. There is a very gradual decrease in $\mu_{\text{eff}}/\text{Fe}$ as the sample is cooled to a plateau where $\mu_{\text{eff}}/\text{Fe} = \text{ca. } 4.4 \mu_{\text{B}}$. The spin-crossover transition occurs even more suddenly in the recrystallized sample compared to the original crystalline sample.

The effect of doping $[\text{Fe}(3\text{-OCH}_3\text{-SalEen})_2]\text{PF}_6$ into the diamagnetic cobalt(III) host is illustrated in Figure 11 (data are given in Tables XIX–XXII⁸). The data show that, as for the chromium(III) case, the transition becomes more gradual as the cobalt(III) concentration is increased. There is one difference, however. Unlike the chromium(III) case, the transition temperature is shifted to a higher temperature as the concentration of cobalt(III) is increased. The ionic radius of high-spin iron(III) ion, $r_{\text{Fe}} = 0.65 \text{ \AA}$, is comparable to the ionic radius of chromium(III) ion, $r_{\text{Cr}} = 0.62 \text{ \AA}$. Doping the iron(III) complexes into the chromium(III) lattice does not greatly affect the temperature at which the spin-crossover transition occurs. Figure 12 shows that the X-ray powder

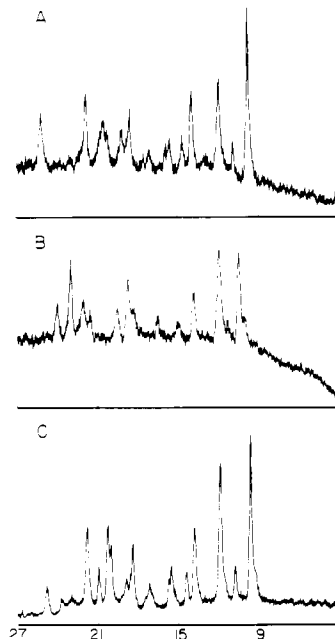


Figure 12. X-ray powder diffraction patterns of $[\text{Fe}(3\text{-OCH}_3\text{-SalEen})_2]\text{PF}_6$ (A), $[\text{Co}(3\text{-OCH}_3\text{-SalEen})_2]\text{PF}_6$ (B), and $[\text{Cr}(3\text{-OCH}_3\text{-SalEen})_2]\text{PF}_6$ (C). A scan rate of 1° of $2\theta/\text{min}$ was employed.

diffraction patterns are almost superimposable for $[\text{Fe}(3\text{-OCH}_3\text{-SalEen})_2]\text{PF}_6$ and $[\text{Cr}(3\text{-OCH}_3\text{-SalEen})_2]\text{PF}_6$. On the other hand, the ionic radius of the cobalt(III) ion, $r_{\text{Co}} = 0.53 \text{ \AA}$, is significantly smaller than the radii for the other two ions. The peaks in the powder pattern of $[\text{Co}(3\text{-OCH}_3\text{-SalEen})_2]\text{PF}_6$ are shifted to higher θ values compared to the corresponding peaks in the pattern for the iron(III) complex. This means that the unit cell of the cobalt(III) complex is smaller than that of the iron(III) complex. When the cobalt(III) complex is used as the host for doping the iron(III) complex, a larger percentage of the iron(III) complexes will be forced into the low-spin state at 286 K than in the pure iron(III) complex. An increase in the concentration of cobalt(III) host is reflected by an increase in the number of low-spin iron(III) complexes. Thus, it appears that the host molecules in a doped system can affect the transition temperature, T_c , in two ways: (1) The role of the host molecules as defects in the lattice tends to lower T_c as the transition becomes more gradual. (2) The ionic radius of the host complex may favor either one of the two spin states. The chromium ion, which is of comparable size to the high-spin ferric ion, has only a minor effect on T_c . The much smaller cobalt ion strongly favors the low-spin state, so T_c is greatly enhanced upon doping in spite of the large number of defects introduced.

As part of our continuing effort to test the generality of the effect of sample grinding, crystalline $[\text{Fe}_{0.77}\text{Co}_{0.23}(3\text{-OCH}_3\text{-SalEen})_2]\text{PF}_6$ was gently ground for 2 min in a mortar and pestle. Figure 13 shows the results. Even a "mild" grinding produces a plateau in the $\mu_{\text{eff}}/\text{Fe}$ vs. temperature curve. The data are given in the Table XXII.⁸ Either the increased sensitivity of doped compounds to grinding could be due to simply the additive effects of grinding and doping or it is possible that a doped compound gives a greater number of defect sites upon grinding.

Doping $[\text{Fe}(\text{SalEen})_2]\text{PF}_6$ into isostructural $[\text{Co}(\text{SalEen})_2]\text{PF}_6$ produced similar, but not as dramatic, changes in the magnetic susceptibility data as observed for the doped $[\text{Fe}(3\text{-OCH}_3\text{-SalEen})_2]\text{PF}_6$ compounds. Tables XXIV–XXVI⁸ give the data, and Figure 14 shows the $\mu_{\text{eff}}/\text{Fe}$ vs. temperature curves. It is seen that for $[\text{Fe}_{0.75}\text{Co}_{0.25}(\text{SalEen})_2]\text{PF}_6$ and $[\text{Fe}_{0.36}\text{Co}_{0.64}(\text{SalEen})_2]\text{PF}_6$ the values of $\mu_{\text{eff}}/\text{Fe}$ are lower than those for the pure compound, as observed for the 3-OCH₃-

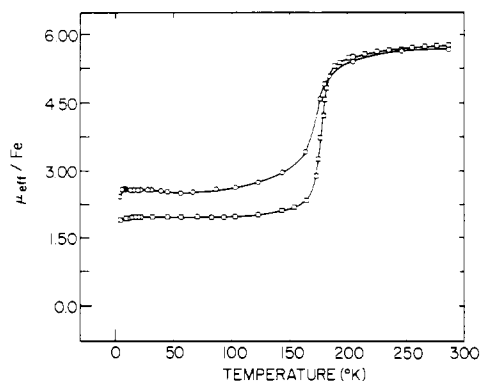


Figure 13. Effective magnetic moment per iron ion ($\mu_{\text{eff}}/\text{Fe}$) vs. temperature curves for $[\text{Fe}_{0.77}\text{Co}_{0.23}(\text{3-OCH}_3\text{-SalEen})_2]\text{PF}_6$: □, unperturbed microcrystalline sample; ○, same solid ground with a mortar and pestle for only 2 min.

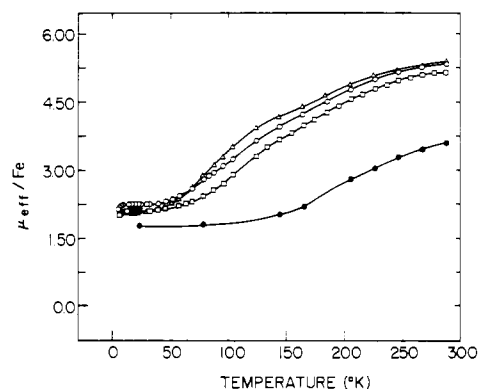


Figure 14. Effective magnetic moment per iron ion ($\mu_{\text{eff}}/\text{Fe}$) vs. temperature for microcrystalline $[\text{Fe}_x\text{Co}_{1-x}(\text{SalEen})_2]\text{PF}_6$: ○, $x = 1$; □, $x = 0.79$; Δ, $x = 0.60$; ●, $x = 0.36$.

SalEen compounds. However, the compound $[\text{Fe}_{0.60}\text{Co}_{0.40}(\text{SalEen})_2]\text{PF}_6$ does not seem to follow the trend. A second sample with this same composition was prepared, and it showed somewhat different characteristics (see Table XXVII); however, it still does not fit into the trend.

Two interesting observations were noted in the EPR spectra of the iron(III) complexes doped in the diamagnetic cobalt(III) host. At room temperature, $[\text{Fe}(\text{3-OCH}_3\text{-SalEen})_2]\text{PF}_6$ shows a low-spin signal at $g \approx 2.0$ and a high-spin signal at $g \approx 7.5$. Doping this complex into the analogous cobalt(III) complex gives a new high-spin signal at $g \approx 5.5$, as can be seen in Figure 15 which shows the spectrum for $[\text{Fe}_x\text{Co}_{1-x}(\text{3-OCH}_3\text{-SalEen})_2]\text{PF}_6$. The intensity of this new signal increases from one doped sample to another as the concentration of cobalt(III) is increased. This just underscores the suggestion made above that the effective system $[\text{Fe}(\text{3-OCH}_3\text{-SalEen})_2]\text{PF}_6$ is unusual and susceptible to changes by grinding and doping.

In the case of $[\text{Fe}(\text{SalEen})_2]\text{PF}_6$, an apparently axial low-spin signal is seen at 77 K with broad "perpendicular" and

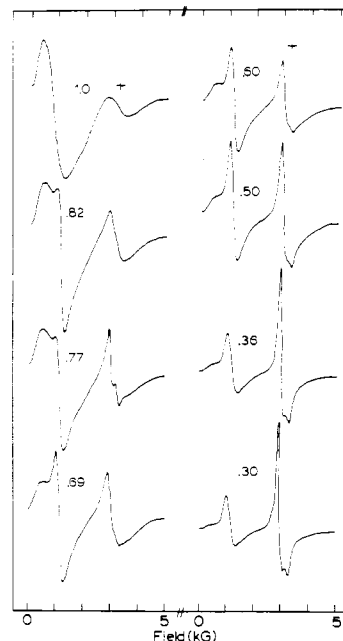


Figure 15. Room-temperature X-band EPR spectra of microcrystalline $[\text{Fe}_x\text{Co}_{1-x}(\text{3-OCH}_3\text{-SalEen})_2]\text{PF}_6$ for various values of x .

"parallel" signals at $g = 2.177$ and 2.015 , respectively. As the cobalt(III) content is increased, it becomes apparent that there really is more than one type of low-spin signal seen. The spectrum of $[\text{Fe}_{0.36}\text{Co}_{0.64}(\text{SalEen})_2]\text{PF}_6$, for example, shows a distorted "derivative" at $g = 2.209$ and "bumps" at $g = 2.140$, 2.009 , and 1.936 .

Conclusion

It has been shown that the changes seen upon grinding or doping of the spin-crossover $[\text{Fe}(\text{X-SalEen})_2]\text{Y}$ compounds are in keeping with the nucleation and growth mechanism of phase transitions in the solid state. Experiments are needed to directly control and monitor the number and nature of crystal defects and domains in these interesting spin-crossover complexes.

Acknowledgment. The support of the National Institutes of Health through Grant HL 13652 is gratefully acknowledged. We are thankful to Professor Peter Debrunner for the use of his Mössbauer instrumentation.

Registry No. $[\text{Co}(\text{3-OCH}_3\text{-SalEen})_2]\text{NO}_3$, 75083-19-1; $[\text{Co}(\text{SalEen})_2]\text{NO}_3$, 75083-21-5; $[\text{Co}(\text{3-OCH}_3\text{-SalEen})_2]\text{PF}_6$, 75083-22-6; $[\text{Co}(\text{SalEen})_2]\text{PF}_6$, 75110-31-5; $[\text{Cr}(\text{3-OCH}_3\text{-SalEen})_2]\text{PF}_6$, 73261-33-3; $[\text{Cr}(\text{SalEen})_2]\text{PF}_6$, 75083-24-8; $[\text{Fe}(\text{3-OCH}_3\text{-SalEen})_2]\text{PF}_6$, 73261-31-1; $[\text{Fe}(\text{SalEen})_2]\text{PF}_6$, 73261-28-6; *N*-ethylethylenediamine, 110-72-5; 3-methoxysalicylaldehyde, 877-22-5; $[\text{Cr}(\text{3-OCH}_3\text{-SalEen})_2]\text{Cl}$, 75110-32-6.

Supplementary Material Available: Tables III–X and XII–XXVII, magnetic susceptibility data (39 pages). Ordering information is given on any current masthead page.